Title: Muscle forces comprise a more sensitive measure of post-stroke movement deficits than joint angles.

Authors: Ariel B. Thomas[1,2], Erienne V. Olesh[1,2], Amelia Adcock[3,4], and Valeriya Gritsenko[1,2]

Affiliations:

[1] Department of Human Performance, Division of Physical Therapy, School of Medicine West Virginia University, Morgantown, WV, 26506

[2] Rockefeller Neuroscience Institute, Department of Neuroscience, West Virginia University, Morgantown, WV, 26506

[3] WVU Center for Teleneurology and Telestroke, Morgantown, WV, 26506

[4] Department of Neurology, School of Medicine, West Virginia University, Morgantown, WV, 26506

Corresponding author: Valeriya Gritsenko, PO Box 9226, One Medical Center Drive, Morgantown, WV, 26505-9226. Phone: (304) 293-7719

Running Head: dynamic assessment of post-stroke reaching

Abstract

Background and Purpose: The whole repertoire of complex human motion is enabled by forces applied by our muscles and controlled by the nervous system. The effect of damage to the nervous system such as stroke on the complex multi-joint motion is difficult to quantify in a meaningful way that informs about the underlying deficit in the neural control of movement. We tested the idea that the disruption in intersegmental coordination after stroke can be quantified with higher sensitivity using metrics based on forces rather than motion. Our study aim was to objectively quantify post-stroke motor deficits using motion capture of stereotypical reaching movements. Our hypothesis is that muscle forces estimated based on active joint torques are a more sensitive measure of post-stroke motor deficits than angular kinematics.

Methods: The motion of twenty-two participants was captured when reaching to virtual targets in a center-out task. We used inverse dynamic analysis to derive muscle torques, which were the result of the neural control signals to muscles to produce the recorded multi-joint movements. We then applied a novel analysis to separate the component of muscle torque related to gravity compensation from that related to motion production. We used the kinematic and dynamic variables derived from motion capture to assess age-related and post- stroke motor deficits.

Results: We found that reaching with the non-dominant arm was accomplished with shoulder and elbow torques that had larger amplitudes and inter-trial variability compared to reaching with the dominant arm. These dominance effects confounded the assessment of post-stroke motor deficits using amplitude and variability metrics. We then identified the metric based on waveform comparison that was insensitive to dominance effects. We used it to show that muscle torques with gravity-related components subtracted were much more sensitive to post-stroke motor deficits compared to measures based on joint angles. Using this metric, it was possible to quantify the extent of individual deficits caused by stroke independently from age-related deficits and dominance effects.

Conclusions: Functional deficits seen in task performance have biomechanical underpinnings, seen only through force-based analysis. Our study has shown that estimating muscle forces that drive motion can quantify with high sensitivity post-stroke deficits in intersegmental coordination. A force-based assessment developed based on this method could help quantify less "observable" deficits in mildly affected stroke patients, such as those classified as asymptomatic via traditional motion-based assessments, but who may still report difficulty moving, increased fatigue, and/or inactivity. Moreover, identifying deficits in the different components of muscle forces may be a way to personalize and standardize intervention and increase the effectiveness of robotic therapy.

Keywords: 3D Arm Movements, Stroke Paresis, Nonlinear Dynamics, Motor Control, Motor Assessment

Introduction

Movement is a complex interplay between forces generated by our muscles under the control of the central nervous system and the environment. Neurological diseases such as stroke damage the neuromuscular mechanisms of movement production. The resulting movement deficits are a major contributing factor to stroke being the leading cause of long-term disability in the United States [1].

The clinical assessment of movement deficits is a primary source of actionable information used to design a personal rehabilitation plan [2,3]. Therefore, the quality and type of information obtained from the assessment dramatically influences the effectiveness of therapeutic intervention. Clinical tests are usually developed and validated to obtain a specific type of information about the quality of movement. For example, the Fugl-Meyer assessment (FMA) is designed to measure the level of impairment by quantifying a patient's ability to control independently individual joints [4]. Other tests, such as Wolf Motor Function Test (WMFT) and the Action Research Arm Test (ARAT), focus on measuring the ability to perform functional tasks [5–7]. These subjective tests have variable responsiveness and predictive validity for detecting effects of therapy for stroke and ceiling effects in patients with mild motor deficits [5,8]. More importantly, recent randomized clinical trials show variable effectiveness of treatments developed based on the evidence provided by these clinical assessments [9–11]. It is widely believed that higher quality evidence for informing the design of future interventions is needed [12,13].

An established way to quantify movement deficits is motion capture. This technology, originally developed for the entertainment industry and widely adopted in research laboratories, is now entering people's homes via gaming controllers. Off-the-shelf motion capture systems suitable for home use have already been used to quantify movement deficits after stroke and shown to be relatable to existing clinical assessments [14–17]. However, measuring kinematic variables, such as movement extent and speed, can provide only indirect information about how the movement is generated by neuromuscular action. It is not possible to infer from kinematic measures what forces were applied by the muscles to make the arm move, even for a seemingly simple but clinically important determination of whether the motion is active or passive. The forces muscles produce can be estimated by inverse modeling using the equations of motion. Motion capture data is used to compute first joint angles in time and then active joint moments, termed angular excursions and muscle torques [18–21]. Muscle torques are rotational forces produced by the summed result of all the forces generated by muscle contractions. This inverse modeling approach takes into account passive forces caused by complex limb inertia and extrinsic forces, such as gravity or objects held in the hand. Thus, muscle torques represent only the active forces necessary to produce the observed motion in presence of all the internal and external passive forces [22–26]. Muscle torques can then be used to quantify changes in active movement caused by stroke, possibly with more sensitivity than that based on joint angles or angular excursions.

Gravity plays an important role in movement control contributing to both posture and movement [27,28]. Unloading the arm against gravity in stroke survivors with hemiparesis has been shown to improve reach distance and grasping performance [18,29,30], while additional loading at the shoulder worsens performance with hemiparetic hand [31]. The additive component of muscle torques responsible for overcoming gravity can be extracted from equations of motion [19,32,33]. This gravitational component of muscle torque depends only on the orientation of limb segment relative to gravity and it is independent of the speed of movement [32,34]. It is thought to be related to the tonic component of muscle activity in different postures [35,36] or as the first

principal component that captures the most variance in muscle activity [33,34]. These gravity-compensating components of muscle activity may also be driven by reticulospinal pathway involved in anticipatory postural adjustments [37–39]. The reticulospinal pathway has been implicated in post-stroke unmasking of flexor synergies involving the antigravity muscles of the arm that are a major contributor to motor deficits [40,41]. This is supported by electrophysiological and anatomical evidence from monkeys [42–44]. Notably, flexion synergies become extension synergies in macaques with lesions in the corticospinal tract when they are suspended upside down [45], implicating that the direction of gravity interacts in some way with the presence of stroke synergies. Therefore, quantifying the gravity-related component of muscle torque may provide valuable insights into the post-stroke disruption of postural mechanisms of movement control.

The remainder of active muscle torques after the subtraction of the gravitational component, termed dynamic component, combines all the moments necessary to produce the observed motion without gravity, e.g. in microgravity environment. This portion of muscle torques has a different temporal profile than that of the gravity component of muscle torque [19,32,33,46]. Studies of multisegmented arm motion with and without gravity have shown that this dynamic component reflects the compensation for intersegmental dynamics [47–50]. Deficits in the compensation for interaction torques have been reported in people with lesions in cerebellum, further supporting the role of the dynamic component of active muscle torques in intersegmental coordination [51]. The dynamic component of muscle torque is thought to be related to the phasic component of muscle activity, which is the remainder after subtraction of the tonic component of muscle activity [33]. Moreover, it has been shown that cerebellar damage preferentially impairs phasic EMG [52]. Therefore, quantifying the dynamic component of muscle torque may provide a method to assess post-stroke disruption in intersegmental coordination.

Our study aim was to quantify objectively post-stroke motor deficits using motion capture of stereotypical reaching movements. Our hypothesis is that muscle forces estimated based on active joint torques are a more sensitive measure of post-stroke motor deficits than angular kinematics. Because of the small sample size and the heterogeneity of our sample, we designed our experiment to make intra-subject comparisons, quantifying the symmetry of movement trajectories between both arms. We then applied a novel analysis that separated muscle torques into components related to gravity compensation and motion production and used these and kinematic measures to quantify motor deficits.

Methods

Participants

Twenty-two human participants were recruited to perform reaching movements to virtual targets with both arms. The participants were divided into three groups, Control, Stroke, and Aged. The Control group (23 ± 1.2 years) included 9 participants without any known neurological or musculoskeletal disorders. The kinematic and torque data from the Control group were reported in Olesh et al. [33]. The Stroke group included 8 participants (58 ± 6.9 years), who have suffered single unilateral ischemic stroke at least three months prior to the experiment (Table 1). Diagnosis was performed by neurologists during hospital admission or following neurological evaluations at Ruby Memorial Hospital. Potential participants were excluded if they could not produce visible movement with their shoulder and elbow, or if they were unable to provide written consent to participate. The Aged group (58 ± 2.4 years) included 5 participants without any known neurological or musculoskeletal disorders, whose age was within the mean ± SD of participants in

the Stroke group. All control participants were right-hand dominant and reported no unrelated movement disorders or significant injuries to their upper extremities. The study and the consent procedure were approved by the Institutional Review Board of West Virginia University (Protocol # 1311129283). All participants provided written consent before participation.

Table 1 about here

Experimental Task

During the experiment, participants reached to virtual targets in a center-out task, as described in detail in Olesh et al. [33] (Fig. 1). The arm was not supported, all movements were unconstrained. Movements were instructed using a virtual reality (VR) software (Vizard by Worldviz) and headset (Oculus Rift), which randomly displayed one of 14 targets, 5 cm in diameter, arranged equidistantly from a center target. A center target was placed in the VR space so that the initial posture of the upper arm was aligned with the trunk (all shoulder angles at 0◦) and the forearm parallel to the floor palm down (elbow angle at 90◦ and wrist at 0◦; Fig. 1A). This minimized both the intertrial variability and inter-subject variability in motion trajectories. For each participant, the distance from the center target to the peripheral targets was scaled to 30% of arm length (anterior acromial point to the distal tip of the index finger). This distance between the central and peripheral targets was on average 20 cm. Our most impaired participants (S7 and S8, Table 1) were unable to reach targets reliably with their contralesional arm. Therefore, the reaching distance for the contralesional arm of these participants was decreased to 15 cm.

Participants were seated and instructed to reach to targets as quickly and as accurately as possible without moving their torso. The torso motion was restrained with Velcro straps attached to the vertical backrest of a chair. The participant's arm was visualized in VR as a "stick figure" connecting the positions of motion capture markers (Fig. 1B) and it moved concurrently with the participant at the temporal resolution of the VR helmet refresh rate (~90 Hz). Index fingertip was shown as a yellow ball, participants were instructed to move it into the center of each target. Individual joint motion of the digits was not tracked; therefore, all participants were instructed to keep palm flat with all fingers extended and wrist pronated (palm down). The arm was not supported during reaching. Participants with stroke wore a finger splint made of polystyrene foam weighing < 10 gram to keep the digits 2-5 extended including at the metacarpophalangeal joints (palm down and open).

Each movement began with the participant's hand in the center target. A movement was cued by the center target changing color from green to red and the appearance of one peripheral green target (Fig. 1B). Upon the detection of index fingertip inside the peripheral target radius, its color changed to red, cueing the participant to return to the central target (Fig. 1A, end of center-out movement). After the participant reached the center target (Fig. 1A, end of return movement), the task reset, the peripheral target disappeared, and a new one appeared after a half-second delay. Movements to each peripheral target location were performed in a randomized order and repeated 15 times with rest breaks after bouts of 70 trials or upon request. Each participant repeated this experiment with both arms in separate sessions on different days.

Data Collection and Processing

All analyses were performed in MATLAB (Mathworks Inc.). Motion capture was recorded during the experiment using an active-marker motion capture system (Impulse by PhaseSpace). The light emitting diodes (active markers, LEDs) were placed according to best practice guidelines on anatomical bony landmarks of the arm and trunk [53]. Motion capture was collected at a rate of 480 frames per second, low pass filtered at 10 Hz and interpolated with a cubic spline (maximum interpolated gap: 0.2 s). Angular excursions were calculated from motion capture using local coordinate systems defined as follows. Six LEDs on the clavicle, sternum, spine and the shoulder of the analyzed arm were used to define the trunk coordinate system. All joint angles were calculated relative to the trunk coordinate system, thus controlling for any change in trunk posture. The orientation of the trunk coordinate system was the same for both arms, therefore the directions of motion about the shoulder flexion/extension and internal/external rotation DOFs were opposite between limbs. They were flipped in the correlative analysis described below. Three LEDs, 2 on the shoulder and 1 on the elbow, were used to define upper arm coordinate system. Three LEDs, 1 on the elbow and 2 on the wrist, were used to define forearm coordinate system. Three LEDs, 2 on the wrist and 1 on the fingertip, were used to define hand coordinate system. The axes of the local coordinate systems were oriented in the same direction for both arms as shown in Fig. 1C. Joint angles were defined as Euler angles that corresponded to five joint degrees of freedom (DOFs) including 3 shoulder DOFs flexion/extension, abduction/adduction, internal/external rotation, 1 elbow DOF flexion/extension, and 1 wrist DOF flexion/extension. In some participants the medial wrist LED was not reliably tracked due to being obscured frequently from camera view by moving body segments. Therefore, wrist pronation/supination DOF was not reliably detected and, thus, excluded from analysis. Wrist abduction/adduction was found to be minimal during these tasks and was likewise not included in the analysis.

The onset and offset of each center-out and return movements were identified from the differentiated trajectory of hand marker (velocity) crossing the threshold of 5% of maximal velocity at the beginning and the end of a given movement. Center-out movements toward one of the peripheral targets were separated from the return movements toward the central target by these events and analyzed as separate movements. The events were verified through visual inspection of the plotted trajectories to correct for unintended or corrective motion around the virtual target. The onset and offset events were used for temporal normalization of kinematic and dynamic profiles prior to averaging. Signals starting 100 ms prior to the onset events were included in the analysis of each movement to capture the full profile of phase-advanced torques. All values included in text are means ± standard deviation across subjects, unless otherwise indicated.

Inverse Dynamics

The arm model was implemented in the Simbody toolbox of MATLAB. The model with 5 DOFs described in Olesh et al. [33] was used to calculate forces at the shoulder, elbow, and wrist joints. Angular excursions for the shoulder, elbow, and wrist, obtained as described above were used to drive the model and simulate the center-out and return movements. The trunk was assumed to be stationary and in line with the world coordinate system (Fig. 1C). The inertia of major limb segments (humerus, radius/ulna, and hand) were modeled as ellipsoids with the long axes and masses scaled to the lengths of individual participants [54]. The segment diameters were kept constant at 10 cm, 6 cm, and 6 cm for upper-arm, forearm, and hand respectively. The short axes of the ellipsoids remained constant across participants. Inverse dynamics simulations using the individually scaled model shown in Fig. 1C were ran in Simulink to obtain active muscle torques. The quality of these simulations was checked by running forward simulations and calculating the

root-mean-squared error (RMSE) between the endpoint trajectories obtained from motion capture and those from forward simulations. The RMSE mean ± standard deviation across participants for Control group was 0.07 ± 0.13 and 1.01 ± 2.21 mm for the right and left arm respectively, for the Aged group it was 0.68 ± 0.59 and 1.10 ± 1.10 mm for the right and left arm respectively, and for the Stroke group it was 2.86 ± 6.61 and 7.29 ± 13.70 mm for the ipsilesional and contralesional arm respectively.

Active muscle torques obtained with inverse simulations were divided into two additive components, termed gravitational and dynamic muscle torques. The gravitational component captured the portion of muscle torque that supports the limb segments against the force of gravity. The dynamic component captured the residual muscle torques related to motion production [19,55]. As described in Olesh et al., to obtain the dynamic torque components, we ran the inverse dynamics simulations with gravity of the physics engine set to zero [33]. To obtain the gravitational torque component, the dynamic torque component was subtracted from the overall active muscle torque obtained from simulations with standard gravity for each DOF.

Figure 1 about here

Statistical Analysis

To estimate the extent of individual deficits, we compared the endpoints accuracy of each participant in Stroke and Aged groups to the normative data from the young controls. Endpoint accuracy was calculated as fingertip distance to the center of the outer targets at the end of the center-out reach phase, described above. Movement time was calculated as the elapsed time between the onsets and offsets of each forward and return movement. This did not incorporate reaction time. Paired t-tests were conducted between mean values across all young controls per movement direction and the corresponding data from the matching side in individuals of the Stroke and Aged groups. Bonferroni correction for multiple comparisons was applied. Data in Results are reported as means ± standard deviation across subjects within each group, unless otherwise described.

Angular kinematic and torque signals were normalized in time using onsets and offsets of each movement and resampled (1000 bins). Intertrial variability was calculated as the standard deviation of repetitions of individual movements toward the same target (n = 15) across the normalized trajectory, and then averaged over time. The individual normalized trajectories were averaged to create a mean signal for each center-out and return movement toward each target for each participant.

Statistical analysis to test three hypotheses was applied to metrics calculated from the time-normalized trajectories. In this analysis, the participants served as their own controls, which reduced inter-subject variability. Mirror movements produced by left and right arms were matched because they were accompanied by the same angular excursions and required contractions of the same muscles to produce them. The first metric was obtained by subtracting the minimum from the maximum of the mean time-normalized trajectory of angular excursions, angular velocity, muscle torques and their dynamic and gravitational components per movement direction, DOF, and participant. The amplitudes of signals from the left (non-dominant) arm were then subtracted from those from the right (dominant) arm for each matched movement. Negative values of this amplitude metric indicated that the movements with the non-dominant limb were associated with higher amplitudes of the corresponding signals. The second metric termed intertrial variance metric was obtained from the same signals by calculating a mean standard deviation across

multiple repetitions of each time-normalized trajectory per movement direction, DOF, and participant. The values from the non-dominant limb were subtracted from those of the dominant limb. Negative values of this intertrial variance metric indicate that movements with the non-dominant limb were associated with higher intertrial variance of the corresponding signal type. The units of the amplitude and intertrial variance metrics matched the units of their respective signals, i.e. radians for angular excursions, radians/second for angular velocity, and Nm for all torque signals. The third metric was calculated as the coefficient of determination (R^2) between time-normalized trajectories of left and right limbs per movement direction, DOF, and participant. The resulting waveform metric ranged between 0 (low symmetry or high asymmetry) and 1 (high symmetry or low asymmetry).

To test the null hypotheses that the metrics are equally sensitive to the severity of post-stroke motor deficits, we applied repeated measures analysis of variance (ANOVA) to each of the three metric types averaged across movement directions per signal type, DOF, and subject. All three ANOVAs were structured the same way with a single between-subject factor Group with 3 levels (Control, Aged, and Stroke) and two within-subject factors Signal with 5 levels (joint angle, angular velocity, muscle torque, dynamic muscle forces, and gravitational muscle forces) and DOF with 5 levels (3 shoulder DOFs flexion/extension, abduction/adduction, internal/external rotation, 1 elbow DOF flexion/extension, and 1 wrist DOF flexion/extension). The ANOVA degrees of freedom (df) of within-subject factors (Direction and DOF) was 24, the df of the interaction between within-subject factors and the between-subject factor (Group) was 48, and the error df was 456 for each of the three ANOVAs. The p-values with Greenhouse-Geisser adjustment for sphericity were used to determine significance of main and interaction effects [56]. Post-hoc analyses were conducted using multicompare functions in Matlab based on the ANOVA model with Sidak correction for multiple comparisons.

To compare the sensitivity of angle- and force-based metrics, we used k-means clustering algorithm to classify participants into one of 2 groups, stroke and non-stroke. The data used for clustering was the waveform metric (R^2 values) based on either angular excursions or dynamic forces for summed across movement directions per DOF. To identify clusters, we used squared Euclidean distance measure with a heuristic approach for cluster center initialization [57]. The reproducibility of cluster assignment was tested by running the algorithm 800 times and reporting the chances of individuals with stroke being misclassified into the cluster with Control and Aged participants.

Figure 2 about here

Results

All but two participants in the stroke group were able to perform the center-out and return movements with matched reach amplitudes and targets positions (Fig. 2A). Young controls were the most accurate with the lowest distance from the center of the virtual target to the end of endpoint trajectory (R: 3.69 ± 0.9 cm and L: 3.72 ± 0.5 cm for right and left respectively), followed by the Aged group (R: 3.06 ± 1.1 cm and L: 3.15 ± 1.0 cm), the ipsilesional arm of the stroke group (4.95 ± 1.5 cm), and the contralesional arm of the stroke group (5.86 ± 1.9 cm). The target accuracy was significantly different from the mean across young controls in one aged participant (A2) for the both arms and in one aged participant (A3) for the dominant arm only (paired t-tests $p < 0.0038$ for all). Reach durations in most aged participants were also prolonged compared to

mean duration of the corresponding arm across young controls (paired t-tests $p < 0.0038$ in A1, A4, and A5 for both arms and A3 for only the dominant arm). This shows that most participants in the Aged group reached slower and with lower accuracy compared to young controls.

Both accuracy and movement speed of the contralesional 'impaired' arm were highly variable across Stroke group participants reflecting the heterogeneity of individual pathologies (Table 1). The mean movement duration ± standard deviation across Stroke group participants was 0.79 ± 0.4 s. Individually, the contralesional reach durations were longer in all but two (S4 and S6) participants with stroke compared to the matching side in young controls (paired t-test $p < 0.0038$ for all). The endpoint accuracy was significantly different from young controls in only one stroke subject (S3, $p < 0.0038$). Of note is that the timing and accuracy measures are confounded by the shorter reach distances of two participants (S7 and S8). Despite these differences, the temporal profiles of angular excursions of most Stroke group participants were similar to those of Control and Aged groups including the stereotypical bell-shaped velocity profiles (Fig. 2B). The largest differences in the movement of the Stroke group participants were observed in the profiles and amplitudes of joint torques (Fig. 2B).

The amplitudes of angular excursions and angular velocity of corresponding mirror movements were similar between left and right arms of Control, most Aged, and some of the Stroke group participants (Fig. 3A, B). However, dominance effects appeared in the torque-based metric in Control and Aged groups. The amplitudes of active muscle torque produced by the non-dominant arm were higher than those produced by the dominant arm in all Control and Aged group participants indicated by negative values of the metric (Fig. 3C, D, E). The larger non-dominant muscle torques cannot be accounted for by increased movement speed; the amplitude of angular velocity was similar between the two limbs (Fig 3B). In the Stroke group, movements of both dominant and non-dominant arms were similar in the amplitudes of angular excursions and angular velocity in most participants, with the exception of smaller excursions with the contralesional arm in S7 and S8 (Fig. 3A) due to reduced reach amplitudes described in Methods. Slower movements with left arm were also observed in S7 (Fig. 3B) when the stroke hemisphere is taken into account S5 (Suppl. Fig. S1). The intersubject variance in the amplitude metric based on joint torques was large when plotted as ipsilesional minus contralesional values (Suppl. Fig. S1). However, it was reduced when plotted as right minus left limb (Fig. 3C, D, and E). Therefore, stroke effects in this metric were confounded by dominance effects. The repeated-measures ANOVA on the amplitude metric had a significant effect of within-subject factors ($F = 18.9$, $p = 2e\text{-}08$) and insignificant interaction with between-subject factor Group ($F = 0.6$, $p = 0.75$), indicating that the differences between limbs in the amplitudes of different signals and DOFs were largely consistent across groups. Post-hoc comparisons have shown that the amplitude metric was not significantly different between groups (Table 2A). However, the amplitude metric based on shoulder and elbow torques was clearly outside the variance of the Control and Aged groups in some Stroke group participants (Fig. 3D, E) and the differences between several DOFs and signal types were significant (Table 2B, C). This indicates that the amplitudes of gravitational and dynamic components produced by the non-dominant arm were larger than those produced by the dominant arm about the shoulder flexion/extension, shoulder abduction/adduction, and elbow flexion/extension DOFs. The stroke effect was largely driven by the dominance effects as seen in the reduced intersubject variance in the amplitude of the dynamic component of muscle torque when plotted right vs. left limb in Figure 3D compared to contralesional vs. ipsilesional limb in Supplementary Figure 1D.

Figure 3 about here

Table 2 about here

The intertrial variance of joint excursions and angular velocity for the corresponding mirror movements were similar between Control, Aged, and most of the Stroke group participants (Fig. 4A, B). Quantifying the dynamic component of muscle torque revealed consistent differences between limbs in the intertrial variance, particularly in Control and Stroke groups (Fig. 4C, D, E). The dynamic components in the non-dominant arm were more variable than those produced by the dominant arm across multiple repetitions of the same mirror movements in most DOFs in all participants. This is likely due to the larger amplitudes of non-dominant torques observed with the amplitude metric in all groups. For the Stroke group, the variability metric was also driven by dominance effects, as intersubject variance in this metric increased greatly when contralesional values were subtracted from ipsilesional values (Suppl. Fig. S2). The repeated-measures ANOVA on the intertrial metric had a significant effect of within-subject factors ($F = 9.74$, $p = 7e\text{-}05$) and insignificant interaction with between-subject factor Group ($F = 0.9$, $p = 0.49$), indicating that the differences between limbs in the intertrial variance were largely consistent across groups. Consequently, post-hoc comparisons have shown that the amplitude metric was not significantly different between groups (Table 3A). However, the differences between DOFs and signal types were significant (Table 3B, C), indicating that the larger shoulder and elbow torques produced by the non-dominant limb were also more variable than those produced by the dominant limb.

Figure 4 about here

Table 3 about here

The waveform metric showed that the profiles of the angular excursions and velocity were highly symmetrical between limbs in the Control and Aged groups and less symmetrical in the Stroke group (Fig. 5A, B). Thus, no dominance effects were observed with this metric. The intersubject variability in Control group and for some DOFs in Aged group was reduced when observed with the dynamic component of muscle torque compared to the overall muscle torque across most DOFs. Therefore, the differences between Control, Aged and Stroke groups were greatly amplified when quantified with the metric based on the dynamic component of muscle torque (Fig. 5D). Interestingly, the waveform metric based on dynamic and gravitational torques for elbow and wrist DOFs in some participants in the Aged group lied outside the Control group variance, suggesting possible age-related motor deficits. Most Stroke group participants were completely outside the intersubject variance of the Control group when quantified with the waveform metric based on the dynamic component of muscle torque. The repeated-measures ANOVA on the waveform metric had a significant effect of within-subject factors ($F = 46.35$, $p = 2e\text{-}29$) and a significant interaction with between-subject factor Group ($F = 2.17$, $p = 0.016$), indicating that the differences between groups quantified by the different kinematic and dynamic signals were not equal. Post-hoc comparisons have shown that the waveform metric was significantly different between Control and Stroke groups (Table 4A). Moreover, the differences between most DOFs and signal types were significant (Table 4B, C), further supporting the conclusion that the different types of signals carry different information about the age-related and post-stroke motor deficits. Specifically, all three metrics based on the dynamic component of muscle torque showed the most consistent differences between limbs and the largest differences

between groups (Fig. 3D, 4D, and 5D). This indicates that the dynamic muscle torque is the most sensitive measure of post-stroke motor deficits compared to the rest of examined signals.

Figure 5 about here

To further test the idea that the dynamic measures are more sensitive to the individual motor deficits due to stroke and able to distinguish those from age-related deficits and dominance effects, we used k-means clustering analysis (see Methods). Individuals with stroke and older healthy individuals both had lower values of waveform metric based on dynamic torque compared to the metric based on angular excursions (Fig. 6A) The clustering analysis showed a larger separation between Stroke group participants and the rest based on dynamic forces compared to that based on angular excursions (Fig. 6B & C). The distance between clusters based on angular excursions was 0.28 ± 0.05, while the distance between clusters based on dynamic forces was 0.39 ± 0.02. Consequently, more individuals were misclassified into the wrong group using joint-angle clustering. The mean chance of participants with stroke being misclassified into the cluster with Control and Aged group participants based on joint-angle clustering was 49%, compared to a 17% chance of them being misclassified based on dynamic torque clustering. The chances of Control group participants being misclassified went down from 18% based on angular excursions to 0% based on dynamic torques. However, the chances of Aged group participants being classified with Stroke group participants increased from 22% based on angular excursions to 42% based on dynamic torques. The increase was specific to the aged participants with higher asymmetricity in their torque profiles (Fig. 6A), indicating that it may be possible to use the waveform metric based on dynamic torques to detect age-related motor deficits. This further supports the conclusion that dynamic muscle torque is the a more sensitive measure of post-stroke and, possibly, age-related motor deficits compared to angular excursions.

Figure 6 about here

Table 4 about here

Discussion

We have objectively quantified post-stroke motor deficits using motion capture of reaching movements in a center-out task. Overall, our results confirm the hypothesis that active joint torques are a more sensitive measure of post-stroke motor deficits than angular kinematics. We observed larger intertrial variability and altered temporal waveforms after stroke, which was most evident in the dynamic component of muscle torque (Fig. 4, 5). These differences were much less pronounced and more variable in metrics based on kinematics. We also observed that quantifying reaching using the components of muscle torque reduced the intersubject variability in control participants compared to kinematic measures and controlled for dominance effects. Therefore, the individual post-stroke and age-related motor deficits could be distinguished from inter-subject variability only using the waveform metric based on the dynamic component of muscle torque. The same result was obtained with clustering analysis (Fig. 6). A force-based assessment developed based on this method could be helpful in quantifying objectively individual motor impairment. This type of assessment may be especially useful for patients who have less "observable" deficits, such as those classified as asymptomatic via traditional motion-based assessments, but who may still report difficulty moving, increased fatigue, and/or inactivity. Technology has advanced to the point where low-cost commercial motion capture devices in

combination with powerful computing devices capable of running sophisticated algorithms are becoming widely available for home use. Our study has shown that estimating muscle forces that drive motion can enable a new type of automated assessment of post-stroke motor deficits. This approach can be potentially useful as part of telemedicine and mobile health initiatives, where the patient's health needs to be monitored remotely, for example during the next pandemic.

The nature of dominance effects in the neural control of movement is hotly debated. Results of studies with planar goal-directed movements that control for the effect of gravity have indicated that the neural compensation for intersegmental dynamics for the non-dominant limb tends to be worse than that for the dominant limb [58–60]. Here we quantified the neural compensation for intersegmental dynamics by estimating the residual component of muscle torque after controlling for the effect of gravity, termed the dynamic component of muscle torque. We found differences between limbs in both peak-to-peak amplitudes, intertrial variability, and waveform shapes of the dynamic component of muscle torque in young and aged control participants (Fig. 3D, 4D, and 5D). These metrics showed that the non-dominant torques about the elbow and shoulder flexion/extension and abduction/adduction DOFs were larger, more variable, and had different profiles compared to the corresponding dominant torques, supporting the published observations. It has also been proposed that, compared to the dominant limb, the non-dominant limb may have more efficient postural control, possibly due to increased reliance on impedance control strategy [58,59,61]. Here we quantified postural control by extracting the component of muscle torque that compensates for the effect of gravity on the limb, termed the gravitational component of muscle torque. We found larger amplitudes of the gravitational component of muscle torque about the elbow and shoulder flexion/extension DOF of the non-dominant limb compared to that of the dominant limb and decreased intersubject variability in this metric for the Control group (Fig. 3E). The intertrial variances and the waveform shapes of the gravitational components were not different between limbs (Fig. 4E, 5E). The gravitational component includes both the contribution of muscle forces to maintaining posture before and after movement and the contribution of muscle forces to the postural transitions during movement. Thus, this variable likely reflects both aspects of the neural control strategy: posture and movement. However, the increase in the amplitude of the gravitational component in the non-dominant limb without the complimentary increase in intertrial variability and without changes in the waveform shape is suggestive of more reliance on impedance control of the non-dominant limb for gravity compensation.

Here we show that torque-based measurement of post-stroke motor deficits is more sensitive to individual pathology compared to motion-based measurements. Our results have shown that the waveform metric based on the dynamic component of muscle torque was the most sensitive in quantifying the post-stroke changes in the force trajectory in individuals while controlling for dominance effects and inter-subject differences (Fig. 5D). In contrast, the waveform metric based on kinematic variables tended to saturate in the mildly impaired stroke participants (Fig. 5A), which is consistent with the observation that most of the recruited participants were able to perform the center-out task without obvious difficulties. Furthermore, the clustering analysis has shown that using the metric based on the dynamic component it was possible to identify all individuals with movement deficits due to stroke compared to only two individuals with stroke using the metric based on angular excursions (Fig. 6). This shows that the force-based measures of individual motor deficits due to stroke are much more sensitive than motion-based measures in quantifying the subtle multi-joint differences in complex 3D reaching movements.

The dynamic component of active muscle torque is indicative of intersegmental coordination, something that cannot be easily inferred from movement observation. Our results have shown that most Stroke group participants show a deficit in this metric. This is consistent with published observations showing deficits in intersegmental coordination and the phasic muscle activity patterns after a stroke during the performance of planar reaching tasks and some unconstrained reaching tasks [51,52,62–64]. Furthermore, our analysis allowed us to separate the effects of stroke on gravity compensation from its effect on intersegmental coordination. Here we observed very small post-stroke deficits in the waveform metric based on the gravitational component of muscle torque in most participants (Fig. 5E). This indicates that different mechanisms may be involved in gravity compensation from those involved in intersegmental coordination and that they may be differently affected by stroke. Our results support this conclusion by showing the different extent of individual deficits measured based on the gravitational and dynamic components of muscle torques. For example, S2 had an outlying waveform metric based on the gravitational component about shoulder abduction/adduction and wrist flexion/extension DOFs, but normal waveform metric based on the dynamic component, while S4 showed the opposite pattern (Fig. 5D, E). Future studies with larger sample sizes will help determine the potential of the separation of torque components for the assessment of different types of post-stroke deficits. A potentially ripe application of the torque separation technique is in robotic or robot-assisted post-stroke rehabilitation [29,65–68]. New approaches for designing the pattern of robot assistance or resistance to appropriately titrate the difficulty of therapy while avoiding moving the arm passively, are needed [69,70]. Identifying deficits in the different active torque components and setting robotic devices to assist or resist these components may be a way to personalize and standardize intervention and increase the effectiveness of robotic therapy.

Motor deficits in the elderly are usually ascribed to sarcopenia [71–74] or non-specific and individual neurological changes [75,76]. The small group of aged participants in our study performed reaching movements very differently from young controls. Most participants in the Aged group did movements slower and with lower accuracy (see Results). Furthermore, several aged participants showed multiple metric values outside the ranges of young controls (Fig. 3,4, and 5). The participants in the Aged group were more likely to be classified with the participants in the Stroke group rather than with the Control group based on our most sensitive metric (Fig. 6). This suggests that the force-based measures may be more sensitive to age-related motor deficits than motion-based measures are. These metrics may enable a more mechanistic assessment of age-related motor deficits in future studies.

Tables

Table 1. Stroke group characteristics.

ID	Gender	Infarct hemi-sphere	Infarct description and location	Age	Years post stroke	Contralesional reach duration (s)	Contralesional endpoint accuracy (cm)
1	F	Left	Left middle cerebral artery	51	3	0.7 ± 0.16	4.5 ± 0.87
2	M	Left	Left caudate lenticular nuclei and external horn of the left ventricle	58	5	0.8± 0.11	4.1 ± 1.22

3	M	Right	Right dorsal pontine-medullary lacunar infarction	67	0.5	0.7 ± 0.17	5.6 ± 1.37
4	M	Right	Lacunar infarct in posterior right putamen and border of right internal capsule	68	0.25	0.5 ± 0.08	4.5 ± 1.04
5	M	Left	Left middle cerebral artery	53	0.5	1.3 ± 0.52	8.2 ± 2.80
6	M	Right	Right middle cerebral artery	60	6	0.5 ± 0.10	4.3 ± 1.37
7	M	Right	Right lateral medullary infarction with occluded right vertebral artery	51	8	1.4± 0.49*	8.6 ± 2.63
8	M	Right	Right middle cerebral artery, extending posteriorly	53	7	0.4± 0.12*	7.2 ± 3.30

* The amplitude of movement in these participants was decreased due to their inability to reach the same distance as controls.

Table 2: Post-hoc comparisons for ANOVA on amplitude metric.

	Difference	**Standard Error**	***p***
A: Comparison between groups			
Aged – Control	0.002	0.069	1.000
Aged – Stroke	0.022	0.071	0.947
Control – Stroke	0.020	0.060	0.939
B: Comparison between DOFs			
Elbow F/E – Shoulder F/E	-0.007	0.050	1.000
Elbow F/E – Shoulder Ab/Ad	-0.161	0.032	**0.001**
Elbow F/E – Shoulder In/Ex	-0.261	0.036	**0.000**
Elbow F/E – Wrist F/E	-0.256	0.034	**0.000**
Shoulder F/E – Shoulder Ab/Ad	-0.154	0.066	0.173
Shoulder F/E – Shoulder In/Ex	-0.254	0.069	0.012
Shoulder F/E – Wrist F/E	-0.250	0.075	0.025
Shoulder Ab/Ad – Shoulder In/Ex	-0.100	0.025	**0.005**
Shoulder Ab/Ad – Wrist F/E	-0.095	0.030	0.037
Shoulder In/Ex rot – Wrist F/E	0.005	0.017	0.998
C: Comparison between signal types			
ANG - TORD	0.381	0.053	**0.000**
ANG - TORG	0.186	0.044	**0.004**
ANG - TORM	0.203	0.037	**0.000**
ANG - VEL	0.047	0.023	0.272
VEL - TORD	0.334	0.052	**0.000**
VEL - TORG	0.139	0.053	0.106
VEL - TORM	0.157	0.047	0.025
TORM - TORD	0.178	0.041	**0.003**
TORM - TORG	-0.017	0.029	0.973
TORD - TORG	-0.195	0.044	**0.002**

F/E stands for flexion/extension; Ab/Ad stands for abduction/adduction; In/Ex stand for internal/external rotation of the shoulder. The significant alpha corrected for repeated measures in A is equal to 0.0170; the corrected alpha in B

and C is equal to 0.0051. ANG stands for angular excursions; VEL stands for angular velocity; TORM stands for muscle torque; TORD stands for the dynamic component of muscle torque; TORG stands for the gravitational component of muscle torque.

Table 3: Post-hoc comparisons for ANOVA on intertrial variance metric.

A: Comparison between groups	**Difference**	**Standard Error**	***p***
Aged – Control	0.004	0.027	0.990
Aged – Stroke	0.040	0.028	0.343
Control – Stroke	0.036	0.024	0.300
B: Comparison between DOFs			
Elbow F/E – Shoulder F/E	0.021	0.020	0.834
Elbow F/E – Shoulder Ab/Ad	0.056	0.017	0.024
Elbow F/E – Shoulder In/Ex	-0.027	0.006	0.004
Elbow F/E – Wrist F/E	-0.036	0.007	**0.001**
Shoulder F/E – Shoulder Ab/Ad	0.035	0.024	0.609
Shoulder F/E – Shoulder In/Ex	-0.048	0.021	0.195
Shoulder F/E – Wrist F/E	-0.057	0.023	0.138
Shoulder Ab/Ad – Shoulder In/Ex	-0.082	0.015	**0.000**
Shoulder Ab/Ad – Wrist F/E	-0.091	0.021	**0.003**
Shoulder In/Ex rot – Wrist F/E	-0.009	0.008	0.763
C: Comparison between signal types			
ANG - TORD	0.064	0.008	**0.000**
ANG - TORG	0.075	0.020	0.009
ANG - TORM	0.091	0.019	**0.001**
ANG - VEL	0.016	0.007	0.222
VEL - TORD	0.048	0.010	**0.001**
VEL - TORG	0.059	0.019	0.040
VEL - TORM	0.075	0.018	**0.004**
TORM - TORD	-0.027	0.018	0.558
TORM - TORG	-0.016	0.004	**0.002**
TORD - TORG	0.011	0.019	0.981

F/E stands for flexion/extension; Ab/Ad stands for abduction/adduction; In/Ex stand for internal/external rotation of the shoulder. The significant alpha corrected for repeated measures in A is equal to 0.0170; the corrected alpha in B and C is equal to 0.0051. ANG stands for angular excursions; VEL stands for angular velocity; TORM stands for muscle torque; TORD stands for the dynamic component of muscle torque; TORG stands for the gravitational component of muscle torque.

Table 4: Post-hoc comparisons for ANOVA on waveform matric.

A: Comparison between groups	**Difference**	**Standard Error**	***p***
Aged – Control	-0.035	0.023	0.310
Aged – Stroke	0.067	0.024	0.027
Control – Stroke	0.102	0.020	**0.000**

B: Comparison between DOFs			
Elbow F/E – Shoulder F/E	-0.007	0.012	**0.000**
Elbow F/E – Shoulder Ab/Ad	-0.161	0.010	**0.000**
Elbow F/E – Shoulder In/Ex	-0.261	0.007	0.233
Elbow F/E – Wrist F/E	-0.256	0.007	**0.000**
Shoulder F/E – Shoulder Ab/Ad	-0.154	0.015	**0.000**
Shoulder F/E – Shoulder In/Ex	-0.254	0.015	**0.000**
Shoulder F/E – Wrist F/E	-0.250	0.015	**0.000**
Shoulder Ab/Ad – Shoulder In/Ex	-0.100	0.012	**0.000**
Shoulder Ab/Ad – Wrist F/E	-0.095	0.012	0.988
Shoulder In/Ex rot – Wrist F/E	0.005	0.009	**0.000**
C: Comparison between group by variable type			
ANG - TORD	0.229	0.013	**0.000**
ANG - TORG	0.116	0.014	**0.000**
ANG - TORM	0.271	0.015	**0.000**
ANG - VEL	0.151	0.012	**0.000**
VEL - TORD	0.078	0.014	**0.000**
VEL - TORG	-0.036	0.019	0.382
VEL - TORM	0.120	0.023	**0.000**
TORM - TORD	-0.041	0.015	0.095
TORM - TORG	-0.155	0.016	**0.000**
TORD - TORG	-0.114	0.015	**0.000**

F/E stands for flexion/extension; Ab/Ad stands for abduction/adduction; In/Ex stand for internal/external rotation of the shoulder. The significant alpha corrected for repeated measures in A is equal to 0.0170; the corrected alpha in B and C is equal to 0.0051. ANG stands for angular excursions; VEL stands for angular velocity; TORM stands for muscle torque; TORD stands for the dynamic component of muscle torque; TORG stands for the gravitational component of muscle torque.

Figure Legends

Figure 1. Standardized reaching in virtual reality. A) Trial timeline for each center-out and return reaching movement toward one of 14 virtual targets. B) Participant's VR view of the targets with visual feedback of their limb position (black "stick figure" indicating hand, forearm, and upper arm), the yellow sphere indicated the position of the tip of the index finger. C) Side view of the scaled dynamic model of the arm for one participant and relative target locations. The checkered circles represent the centers of mass of the segments. Arrows represent the orientations of local and world coordinate systems used for defining joint angles and the degrees of freedom for the right arm. Shoulder, elbow, and wrist flexion/extension degrees of freedom were calculated around X (red) axes. Shoulder abduction/adduction degree of freedom was calculated around Y (green) axis. Shoulder internal/external rotation degree of freedom was calculated around Z (blue) axis. The relative target locations are shown for all movement directions. The model posture shows a moment in time during the dynamic simulation of a reaching movement from the center target to the peripheral target 11 (movement up).

Figure 2. Kinematic and torque profiles of a stroke participant (S4) reaching in the VR center-out task. Profiles for both arms, ipsilesional and contralesional (impaired) to stroke hemisphere, are shown. A) Endpoint trajectories for individual center-out (black) and return to center (purple) reaching movement toward each of 14 peripheral targets. B) Example mean kinematic and dynamic trajectories from one movement. Mean trajectories (lines) and standard deviations (shaded areas) are shown for shoulder flexion/extension DOF for center-out movement to Target 3 (forward, horizontal plane) for the contralesional (impaired, blue) and ipsilesional (yellow) arms.

Figure 3. Amplitude metric across limbs. For the Control and Aged groups, the values for the non-dominant limb were subtracted from the values for the dominant limb. For the Stroke group, the values for the left limb were subtracted from the values for the right limb. Bars show the average difference between limbs across subjects; symbols show values for individual participants. Significantly different group comparisons due to non-overlapping confidence intervals from ANOVA model are marked by asterisks. The amplitude metric calculated based on angular excursions is shown in A, angular velocity in B, muscle torque in C, the gravitational component of muscle torque in D, and the dynamic component of muscle torque in E. Flex/ext indicates flexion and extension DOF, abd/add indicates abduction and adduction DOF, int/ext indicates internal and external rotation. Stroke group participant IDs match those in Table 1.

Figure 4. Intertrial variance metric across limbs. The formatting of plots is as in Fig. 3.

Figure 5. Waveform differences across limbs. The formatting of plots is as in Fig. 3.

Figure 6. Cluster analysis of waveform metric based on angular excursions and dynamic component of muscle torque. A. Waveform metric based on angular excursions and based on the dynamic component of muscle torques averaged across movement directions. The central tendencies of data per subject are shown as means (dark circles) with standard deviation across DOFs (light bars). B. & C. Clustering of the waveform metric based on angular excursions (C) and the dynamic component of muscle torque (D) averaged across all movement directions. Only 2 DOFs are plotted, but the cluster analysis was applied to all 5 DOFs.

Acknowledgments

We thank the study participants for generously giving their time, and M. Powers for her assistance with participant recruitment and the general support of the study; we acknowledge the technical support expertly provided by B. Pollard; we are thankful for insightful and critical comments of S. Yakovenko.

Funding

VG was supported by grants P20GM109098 and P30GM103503 from the National Institute of General Medical Sciences (https://www.nigms.nih.gov). ABT was supported by the training grant T32AG052375 from the National Institute of General Medical Sciences. EVO was supported by a training grant T32GM081741 from the National Institute of General Medical Sciences. AA was supported by grant U54GM104942 from the National Institute of General Medical Sciences. The funders had no role in study design, data collection and analysis, decision to publish, or preparation of the manuscript.

Disclosures

None

References

1. Benjamin EJ, Muntner P, Alonso A, Bittencourt MS, Callaway CW, Carson AP, et al. Heart Disease and Stroke Statistics—2019 Update: A Report From the American Heart Association. Circulation. 2019;139. doi:10.1161/CIR.0000000000000659

2. Carr JH, Shepherd RB. Movement Science: Foundations for Physical Therapy in Rehabilitation. Aspen Publishers; 2000.

3. Sullivan JE, Crowner BE, Kluding PM, Nichols D, Rose DK, Yoshida R, et al. Outcome Measures for Individuals With Stroke: Process and Recommendations From the American Physical Therapy Association Neurology Section Task Force. Phys Ther. 2013;93: 1383–1396. doi:10.2522/ptj.20120492

4. Fugl-Meyer AR, Jääskö L, Leyman I, Olsson S, Steglind S. The post-stroke hemiplegic patient. 1. a method for evaluation of physical performance. Scand J Rehabil Med. 1975;7: 13–31.

5. van der Lee J, Beckerman H, Lankhorst G, Bouter L. The responsiveness of the Action Research Arm and the Fugl-Meyer Assessment Scale in Chronic Storke Patients. Journal of Rehabilitation Medicine. 2001;33: 110–113. doi:10.1080/165019701750165916

6. Wolf SL, Catlin PA, Ellis M, Archer AL, Morgan B, Piacentino A. Assessing Wolf Motor Function Test as Outcome Measure for Research in Patients After Stroke. Stroke. 2001;32: 1635–1639. doi:10.1161/01.STR.32.7.1635

7. Yozbatiran N, Der-Yeghiaian L, Cramer SC. A Standardized Approach to Performing the Action Research Arm Test. Neurorehabil Neural Repair. 2008;22: 78–90. doi:10.1177/1545968307305353

8. Hsieh Y, Wu C, Lin K, Chang Y, Chen C, Liu J. Responsiveness and Validity of Three Outcome Measures of Motor Function After Stroke Rehabilitation. Stroke. 2009;40: 1386–1391. doi:10.1161/STROKEAHA.108.530584

9. Duncan P, Studenski S, Richards L, Gollub S, Lai SM, Reker D, et al. Randomized Clinical Trial of Therapeutic Exercise in Subacute Stroke. Stroke. 2003;34: 2173–2180. doi:10.1161/01.STR.0000083699.95351.F2

10. Saposnik G, Cohen LG, Mamdani M, Pooyania S, Ploughman M, Cheung D, et al. Efficacy and safety of non-immersive virtual reality exercising in stroke rehabilitation (EVREST): a randomised, multicentre, single-blind, controlled trial. The Lancet Neurology. 2016;15: 1019–1027. doi:10.1016/S1474-4422(16)30121-1

11. Wolf SL, Thompson PA, Winstein CJ, Miller JP, Blanton SR, Nichols-Larsen DS, et al. The EXCITE stroke trial: comparing early and delayed constraint-induced movement therapy. Stroke. 2010;41: 2309–2315. doi:10.1161/STROKEAHA.110.588723

12. Krakauer JW, Carmichael ST. Broken Movement: The Neurobiology of Motor Recovery After Stroke. MIT Press; 2017.

13. Pollock A, Farmer SE, Brady MC, Langhorne P, Mead GE, Mehrholz J, et al. Interventions for improving upper limb function after stroke. Cochrane Database Syst Rev. 2014; CD010820. doi:10.1002/14651858.CD010820.pub2

14. Chang Y-J, Chen S-F, Huang J-D. A Kinect-based system for physical rehabilitation: A pilot study for young adults with motor disabilities. Research in Developmental Disabilities. 2011;32: 2566–2570. doi:10.1016/j.ridd.2011.07.002

15. Clark RA, Pua Y-H, Bryant AL, Hunt MA. Validity of the Microsoft Kinect for providing lateral trunk lean feedback during gait retraining. Gait & Posture. 2013;38: 1064–1066. doi:10.1016/j.gaitpost.2013.03.029

16. Mousavi Hondori H, Khademi M. A Review on Technical and Clinical Impact of Microsoft Kinect on Physical Therapy and Rehabilitation. Journal of Medical Engineering. 2014;2014: 1–16. doi:10.1155/2014/846514

17. Olesh EV, Yakovenko S, Gritsenko V. Automated Assessment of Upper Extremity Movement Impairment due to Stroke. Sutherland R, editor. PLoS ONE. 2014;9: e104487. doi:10.1371/journal.pone.0104487

18. Ellis MD, Sukal-Moulton TM, Dewald JPA. Impairment-Based 3-D Robotic Intervention Improves Upper Extremity Work Area in Chronic Stroke: Targeting Abnormal Joint Torque Coupling With Progressive Shoulder Abduction Loading. IEEE Trans Robot. 2009;25: 549–555. doi:10.1109/TRO.2009.2017111

19. Russo M, D'Andola M, Portone A, Lacquaniti F, D'Avella A. Dimensionality of joint torques and muscle patterns for reaching. Frontiers in computational neuroscience. 2014;8: 1–21. doi:10.3389/fncom.2014.00024

20. Sainburg RL, Ghilardi MF, Poizner H, Ghez C. Control of limb dynamics in normal subjects and patients without proprioception. Journal of Neurophysiology. 1995;73: 820–835. doi:10.1152/jn.1995.73.2.820

21. Shabbott BA, Sainburg RL. Differentiating Between Two Models of Motor Lateralization. Journal of Neurophysiology. 2008;100: 565–575. doi:10.1152/jn.90349.2008

22. Dounskaia N, Wang W. A preferred pattern of joint coordination during arm movements with redundant degrees of freedom. Journal of Neurophysiology. 2014;112: 1040–1053. doi:10.1152/jn.00082.2014

23. Gentili R, Cahouet V, Papaxanthis C. Motor planning of arm movements is direction-dependent in the gravity field. Neuroscience. 2007;145: 20–32. doi:10.1016/j.neuroscience.2006.11.035

24. Le Seac'h AB, McIntyre J. Multimodal reference frame for the planning of vertical arms movements. Neuroscience Letters. 2007;423: 211–215. doi:10.1016/j.neulet.2007.07.034

25. Papaxanthis C, Pozzo T, McIntyre J. Kinematic and dynamic processes for the control of pointing movements in humans revealed by short-term exposure to microgravity. Neuroscience. 2005;135: 371–383. doi:10.1016/j.neuroscience.2005.06.063

26. Wang W, Dounskaia N. Neural control of arm movements reveals a tendency to use gravity to simplify joint coordination rather than to decrease muscle effort. Neuroscience. 2016;339: 418–432. doi:10.1016/j.neuroscience.2016.10.009

27. Lackner JR, DiZio P. Human orientation and movement control in weightless and artificial gravity environments. Experimental Brain Research. 2000;130: 2–26. doi:10.1007/s002210050002

28. Pozzo T, Papaxanthis C, Stapley P, Berthoz A. The sensorimotor and cognitive integration of gravity. Brain Research Reviews. 1998;28: 92–101. doi:10.1016/S0165-0173(98)00030-7

29. Sanchez RJ, Liu J, Rao S, Shah P, Smith R, Rahman T, et al. Automating Arm Movement Training Following Severe Stroke: Functional Exercises With Quantitative Feedback in a Gravity-Reduced Environment. IEEE Transactions on Neural Systems and Rehabilitation Engineering. 2006;14: 378–389. doi:10.1109/TNSRE.2006.881553

30. Sukal TM, Ellis MD, Dewald JPA. Shoulder abduction-induced reductions in reaching work area following hemiparetic stroke: neuroscientific implications. Exp Brain Res. 2007;183: 215–223. doi:10.1007/s00221-007-1029-6

31. Lan Y, Yao J, Dewald JPA. The Impact of Shoulder Abduction Loading on Volitional Hand Opening and Grasping in Chronic Hemiparetic Stroke. Neurorehabil Neural Repair. 2017;31: 521–529. doi:10.1177/1545968317697033

32. Hollerbach JM, Flash T. Dynamic interactions between limb segments during planar arm movement. Biol Cybern. 1982;44: 67–77. doi:10.1007/BF00353957

33. Olesh E V, Pollard BS, Gritsenko V. Gravitational and Dynamic Components of Muscle Torque Underlie Tonic and Phasic Muscle Activity during Goal-Directed Reaching. Frontiers in human neuroscience. 2017;11: 1–12. doi:10.3389/fnhum.2017.00474

34. Flanders M, Herrmann U. Two components of muscle activation: scaling with the speed of arm movement. Journal of Neurophysiology. 1992;67: 931–943. doi:10.1152/jn.1992.67.4.931

35. Buneo CA, Soechting JF, Flanders M. Muscle activation patterns for reaching: the representation of distance and time. Journal of Neurophysiology. 1994;71: 1546–1558. doi:10.1152/jn.1994.71.4.1546

36. Flanders M, Pellegrini JohnJ, Geisler ScottD. Basic features of phasic activation for reaching in vertical planes. Exp Brain Res. 1996;110. doi:10.1007/BF00241376

37. Schepens B, Stapley P, Drew T. Neurons in the Pontomedullary Reticular Formation Signal Posture and Movement Both as an Integrated Behavior and Independently. Journal of Neurophysiology. 2008;100: 2235–2253. doi:10.1152/jn.01381.2007

38. Schepens B, Drew T. Independent and Convergent Signals From the Pontomedullary Reticular Formation Contribute to the Control of Posture and Movement During Reaching in the Cat. Journal of Neurophysiology. 2004;92: 2217–2238. doi:10.1152/jn.01189.2003

39. Schepens B, Drew T. Descending Signals From the Pontomedullary Reticular Formation Are Bilateral, Asymmetric, and Gated During Reaching Movements in the Cat. Journal of Neurophysiology. 2006;96: 2229–2252. doi:10.1152/jn.00342.2006

40. Ellis MD, Acosta AM, Yao J, Dewald JPA. Position-dependent torque coupling and associated muscle activation in the hemiparetic upper extremity. Exp Brain Res. 2007;176: 594–602. doi:10.1007/s00221-006-0637-x

41. Ellis MD, Drogos J, Carmona C, Keller T, Dewald JPA. Neck rotation modulates flexion synergy torques, indicating an ipsilateral reticulospinal source for impairment in stroke. Journal of Neurophysiology. 2012;108: 3096–3104. doi:10.1152/jn.01030.2011

42. Isa T, Ohki Y, Alstermark B, Pettersson L-G, Sasaki S. Direct and Indirect Cortico-Motoneuronal Pathways and Control of Hand/Arm Movements. Physiology. 2007;22: 145–152. doi:10.1152/physiol.00045.2006

43. Maier MA, Olivier E, Baker SN, Kirkwood PA, Morris T, Lemon RN. Direct and indirect corticospinal control of arm and hand motoneurons in the squirrel monkey (Saimiri sciureus). J Neurophysiol. 1997;78: 721–733. doi:10.1152/jn.1997.78.2.721

44. Zaaimi B, Edgley SA, Soteropoulos DS, Baker SN. Changes in descending motor pathway connectivity after corticospinal tract lesion in macaque monkey. Brain. 2012;135: 2277–2289. doi:10.1093/brain/aws115

45. Denny-Brown DE, Gilman S, Van der Meulen J. Patterns of cortical ablations leading to dystonic postures. Trans Am Neurol Assoc. 1964;89: 117–121.

46. Hirashima M, Ohgane K, Kudo K, Hase K, Ohtsuki T. Counteractive Relationship Between the Interaction Torque and Muscle Torque at the Wrist Is Predestined in Ball-Throwing. Journal of Neurophysiology. 2003;90: 1449–1463. doi:10.1152/jn.00220.2003

47. Debicki DB, Gribble PL. Persistence of inter-joint coupling during single-joint elbow flexions after shoulder fixation. Exp Brain Res. 2005;163: 252–257. doi:10.1007/s00221-005-2229-6

48. Gribble PL, Ostry DJ. Compensation for Interaction Torques During Single- and Multijoint Limb Movement. Journal of Neurophysiology. 1999;82: 2310–2326. doi:10.1152/jn.1999.82.5.2310

49. Ketcham CJ, Dounskaia NV, Stelmach GE. Multijoint movement control: the importance of interactive torques. Progress in Brain Research. Elsevier; 2004. pp. 207–218. doi:10.1016/S0079-6123(03)43021-5

50. Pigeon P, Bortolami SB, DiZio P, Lackner JR. Coordinated Turn-and-Reach Movements. I. Anticipatory Compensation for Self-Generated Coriolis and Interaction Torques. Journal of Neurophysiology. 2003;89: 276–289. doi:10.1152/jn.00159.2001

51. Bastian AJ, Martin TA, Keating JG, Thach WT. Cerebellar ataxia: abnormal control of interaction torques across multiple joints. Journal of Neurophysiology. 1996;76: 492–509. doi:10.1152/jn.1996.76.1.492

52. Manto M-U, Bosse P. Directional tuning of speed-related activation for reaching in the vertical plane in cerebellar ataxia. Neurological Research. 2003;25: 434–444. doi:10.1179/016164103101201715

53. Robertson G, Caldwell G, Hamill J, Kamen G, Whittlesey S. Research Methods in Biomechanics, 2E. Human Kinetics; 2013.

54. Winter DA. Biomechanics and Motor Control of Human Movement. 4th ed. Hoboken, New Jersey: John Wiley & Sons; 2009.

55. Gottlieb GL, Song Q, Almeida G, Hong DA, Corcos D. Directional control of planar human arm movement. Journal of Neurophysiology. 1997;78: 2985–2998.

56. Geisser S, Greenhouse SW. An Extension of Box's Results on the Use of the Distribution in Multivariate Analysis. The Annals of Mathematical Statistics. 1958;29: 885–891.

57. Arthur D, Vassilvitskii S. K-Means++: the Advantages of Careful Seeding. Proc ACM-SIAM symposium on discrete algorithms. 2007. doi:10.1145/1283383.1283494

58. Bagesteiro LB, Sainburg RL. Handedness: Dominant Arm Advantages in Control of Limb Dynamics. Journal of Neurophysiology. 2002;88: 2408–2421. doi:10.1152/jn.00901.2001

59. Sainburg RL. Evidence for a dynamic-dominance hypothesis of handedness. Exp Brain Res. 2002;142: 241–258. doi:10.1007/s00221-001-0913-8

60. Sainburg RL, Kalakanis D. Differences in Control of Limb Dynamics During Dominant and Nondominant Arm Reaching. Journal of Neurophysiology. 2000;83: 2661–2675. doi:10.1152/jn.2000.83.5.2661

61. Schabowsky CN, Hidler JM, Lum PS. Greater reliance on impedance control in the nondominant arm compared with the dominant arm when adapting to a novel dynamic environment. Exp Brain Res. 2007;182: 567–577. doi:10.1007/s00221-007-1017-x

62. Beer RF, Dewald JPA, Rymer WZ. Deficits in the coordination of multijoint arm movements in patients with hemiparesis: evidence for disturbed control of limb dynamics. Experimental Brain Research. 2000;131: 305–319. doi:10.1007/s002219900275

63. Cirstea MC, Mitnitski AB, Feldman AG, Levin MF. Interjoint coordination dynamics during reaching in stroke. Experimental Brain Research. 2003;151: 289–300. doi:10.1007/s00221-003-1438-0

64. Levin MF. Interjoint coordination during pointing movements is disrupted in spastic hemiparesis. Brain. 1996;119: 281–293. doi:10.1093/brain/119.1.281

65. Patton JL, Stoykov ME, Kovic M, Mussa-Ivaldi FA. Evaluation of robotic training forces that either enhance or reduce error in chronic hemiparetic stroke survivors. Exp Brain Res. 2006;168: 368–383. doi:10.1007/s00221-005-0097-8

66. Volpe BT, Krebs HI, Hogan N, Edelsteinn L, Diels CM, Aisen ML. Robot training enhanced motor outcome in patients with stroke maintained over 3 years. Neurology. 1999;53: 1874–1874. doi:10.1212/WNL.53.8.1874

67. Volpe BT, Krebs HI, Hogan N, Edelstein L, Diels C, Aisen M. A novel approach to stroke rehabilitation: Robot-aided sensorimotor stimulation. Neurology. 2000;54: 1938–1944. doi:10.1212/WNL.54.10.1938

68. Volpe BT, Krebs HI, Hogan N. Is robot-aided sensorimotor training in stroke rehabilitation a realistic option?: Current Opinion in Neurology. 2001;14: 745–752. doi:10.1097/00019052-200112000-00011

69. Kahn LE, Lum PS, Rymer WZ, Reinkensmeyer DJ. Robot-assisted movement training for the stroke-impaired arm: Does it matter what the robot does? Journal of rehabilitation research and development. 2014;43: 619–630.

70. Lum P, Reinkensmeyer D, Mahoney R, Rymer WZ, Burgar C. Robotic Devices for Movement Therapy After Stroke: Current Status and Challenges to Clinical Acceptance. Topics in Stroke Rehabilitation. 2002;8: 40–53. doi:10.1310/9KFM-KF81-P9A4-5WW0

71. Dutta C, Hadley EC. The Significance of Sarcopenia in Old Age. The Journals of Gerontology Series A: Biological Sciences and Medical Sciences. 1995;50A: 1–4. doi:10.1093/gerona/50A.Special_Issue.1

72. Edström E, Altun M, Bergman E, Johnson H, Kullberg S, Ramírez-León V, et al. Factors contributing to neuromuscular impairment and sarcopenia during aging. Physiology & Behavior. 2007;92: 129–135. doi:10.1016/j.physbeh.2007.05.040

73. Evans WJ. What Is Sarcopenia? The Journals of Gerontology Series A: Biological Sciences and Medical Sciences. 1995;50A: 5–8. doi:10.1093/gerona/50A.Special_Issue.5

74. Evans WJ, Campbell WW. Sarcopenia and Age-Related Changes in Body Composition and Functional Capacity. The Journal of Nutrition. 1993;123: 465–468. doi:10.1093/jn/123.suppl_2.465

75. Seidler RD, Bernard JA, Burutolu TB, Fling BW, Gordon MT, Gwin JT, et al. Motor control and aging: Links to age-related brain structural, functional, and biochemical effects. Neuroscience & Biobehavioral Reviews. 2010;34: 721–733. doi:10.1016/j.neubiorev.2009.10.005

76. Shaffer SW, Harrison AL. Aging of the Somatosensory System: A Translational Perspective. Physical Therapy. 2007;87: 193–207. doi:10.2522/ptj.20060083

Figure 1

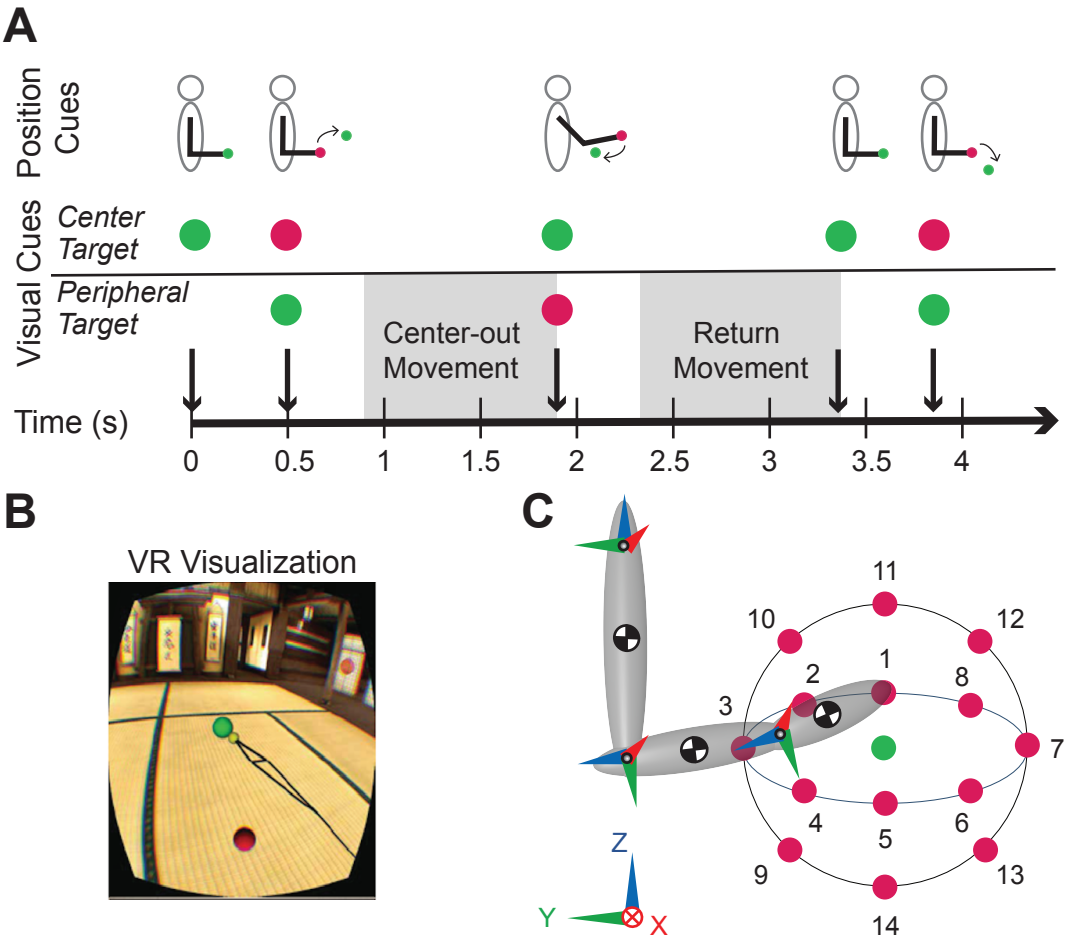
A
Position Cues
Visual Cues
Center Target
Peripheral Target
Center-out Movement
Return Movement
Time (s)
0
0.5
1
1.5
2
2.5
3
3.5
4
B
VR Visualization
C
1
2
3
4
5
6
7
8
9
10
11
12
13
14
Z
Y
X

Figure 2

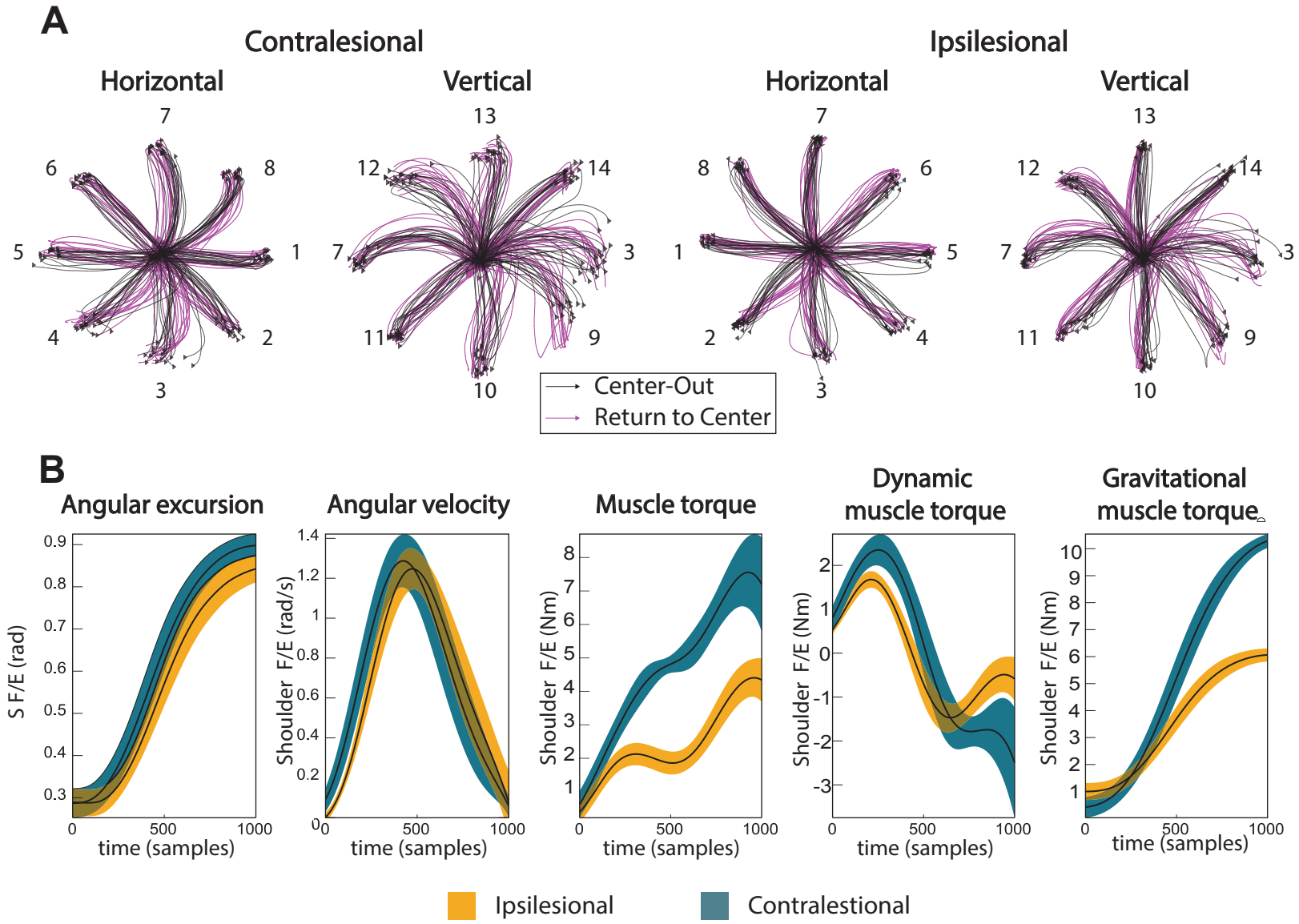
A
Contralesional
Ipsilesional
Horizontal
Vertical
Horizontal
Vertical
Center-Out
Return to Center
B
Angular excursion
Angular velocity
Muscle torque
Dynamic muscle torque
Gravitational muscle torque
S F/E (rad)
Shoulder F/E (rad/s)
Shoulder F/E (Nm)
time (samples)
Ipsilesional
Contralestional

Figure 3

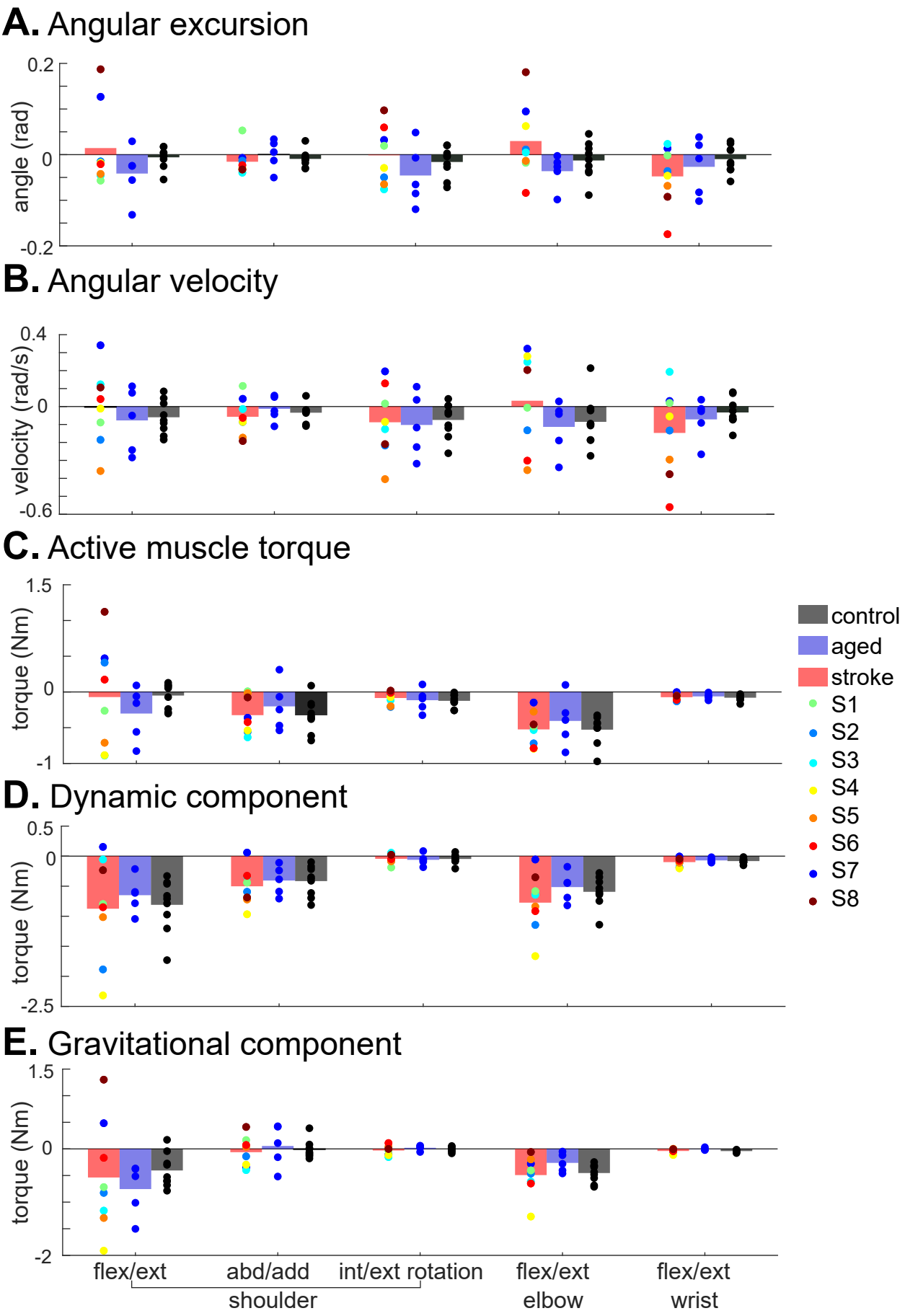
A. Angular excursion
angle (rad)
0.2
0
-0.2
B. Angular velocity
velocity (rad/s)
0.4
0
-0.6
C. Active muscle torque
torque (Nm)
1.5
0
-1
D. Dynamic component
torque (Nm)
0.5
0
-2.5
E. Gravitational component
torque (Nm)
1.5
0
-2
control
aged
stroke
S1
S2
S3
S4
S5
S6
S7
S8
flex/ext
abd/add
int/ext rotation
shoulder
flex/ext
elbow
flex/ext
wrist

Figure 4

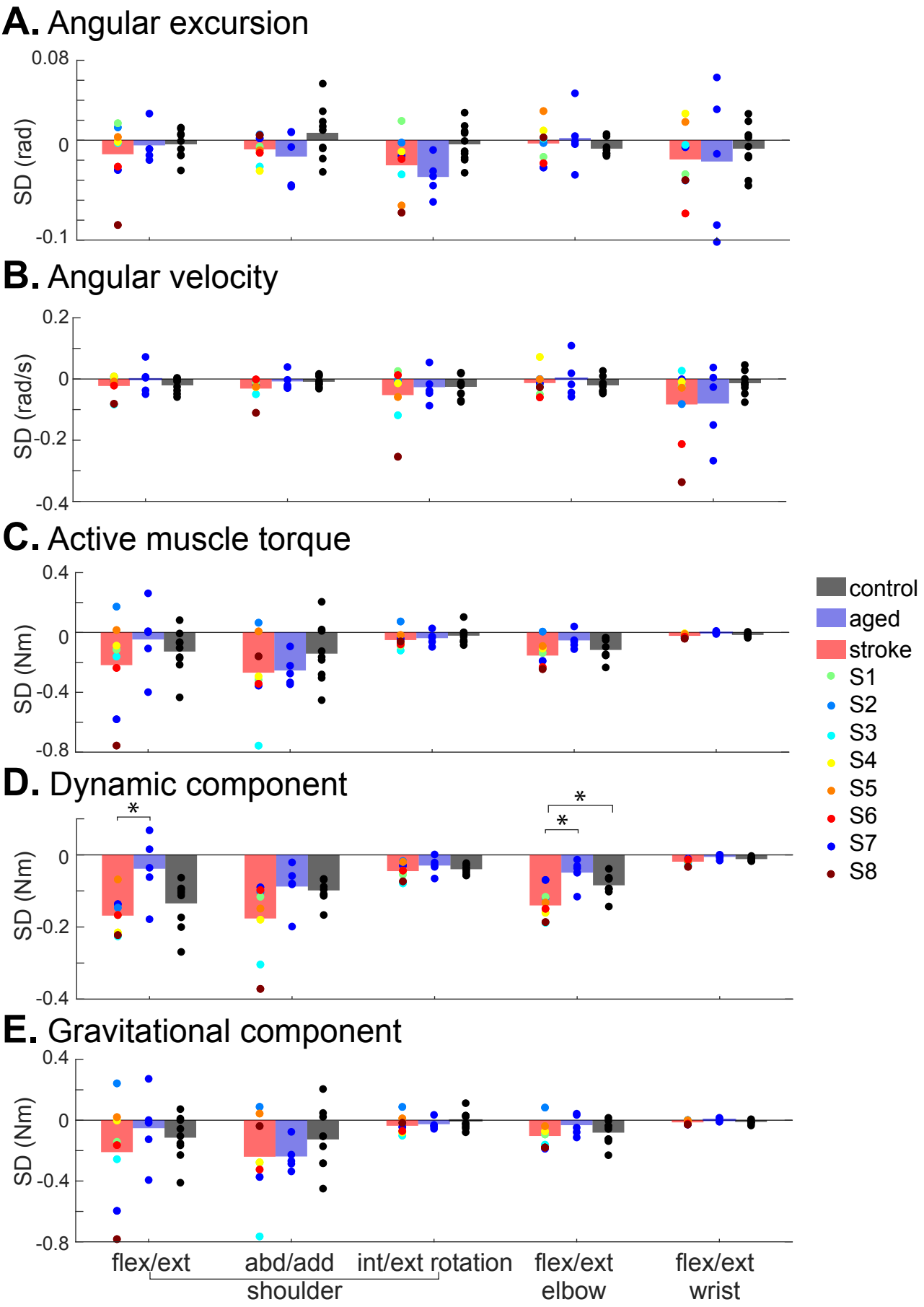
A. Angular excursion
SD (rad)
0.08
0
-0.1
B. Angular velocity
SD (rad/s)
0.2
0
-0.2
-0.4
C. Active muscle torque
SD (Nm)
0.4
0
-0.4
-0.8
D. Dynamic component
SD (Nm)
0
-0.2
-0.4
*
*
*
E. Gravitational component
SD (Nm)
0.4
0
-0.4
-0.8
flex/ext
abd/add
int/ext rotation
shoulder
flex/ext
elbow
flex/ext
wrist
control
aged
stroke
S1
S2
S3
S4
S5
S6
S7
S8

Figure 5

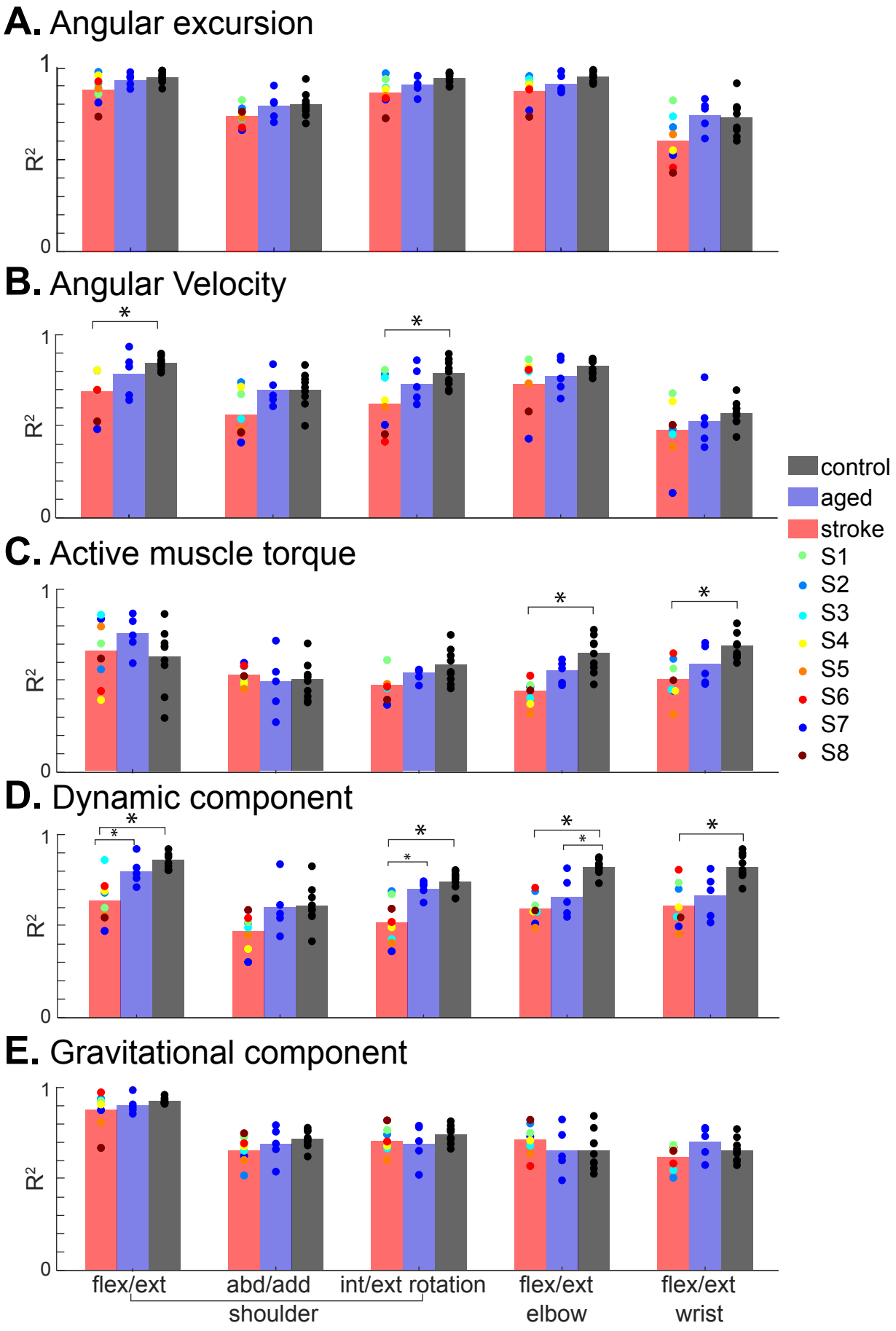
A. Angular excursion
B. Angular Velocity
C. Active muscle torque
D. Dynamic component
E. Gravitational component
R²
1
0
*
control
aged
stroke
S1
S2
S3
S4
S5
S6
S7
S8
flex/ext
abd/add
int/ext rotation
shoulder
flex/ext
elbow
flex/ext
wrist

Figure 6

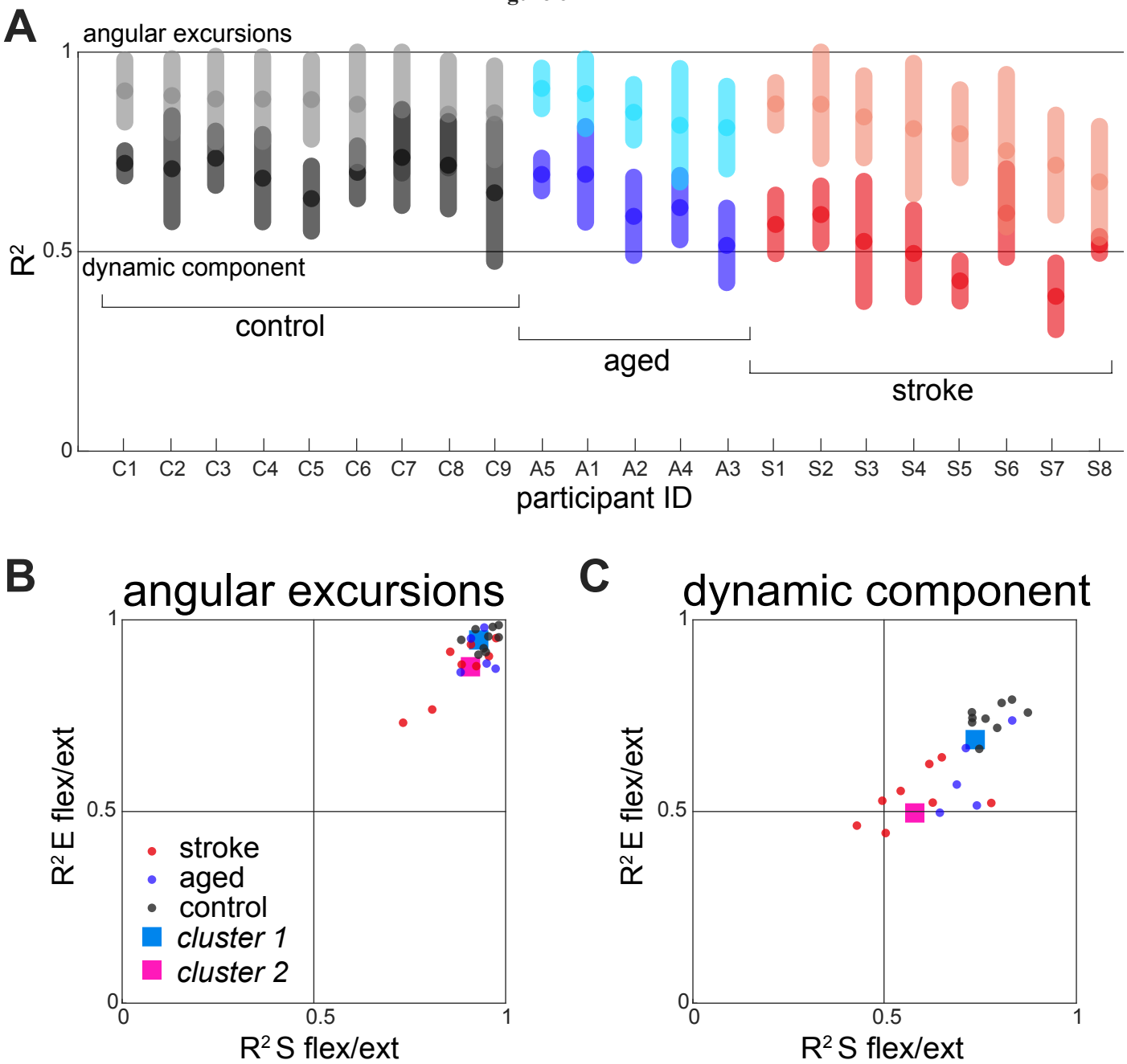
A
angular excursions
dynamic component
R2
1
0.5
0
control
aged
stroke
C1 C2 C3 C4 C5 C6 C7 C8 C9 A5 A1 A2 A4 A3 S1 S2 S3 S4 S5 S6 S7 S8
participant ID
B
angular excursions
R2 E flex/ext
R2 S flex/ext
stroke
aged
control
cluster 1
cluster 2
C
dynamic component
R2 E flex/ext
R2 S flex/ext

Supporting Information

The amplitude metric described in Methods was compared differently between limbs of the Stroke group participants. For the Control and Aged groups, the values for the non-dominant limb were subtracted from the values for the dominant limb as shown in Fig. 3. For the Stroke group, the values for the limb contralesional to stroke (more affected) were subtracted from the values for the ipsilesional limb (less affected). This resulted in less inter-subject variance within the Stroke group in the amplitude metric based on angular velocity of the shoulder flexion/extension (Suppl. Fig. S1) compared to left vs. right comparisons (Fig. 3), but not in other variables. This also shows that the movements of the contralesional arm were always slower than the movements of the ipsilesional arm (Suppl. Fig. 1B).

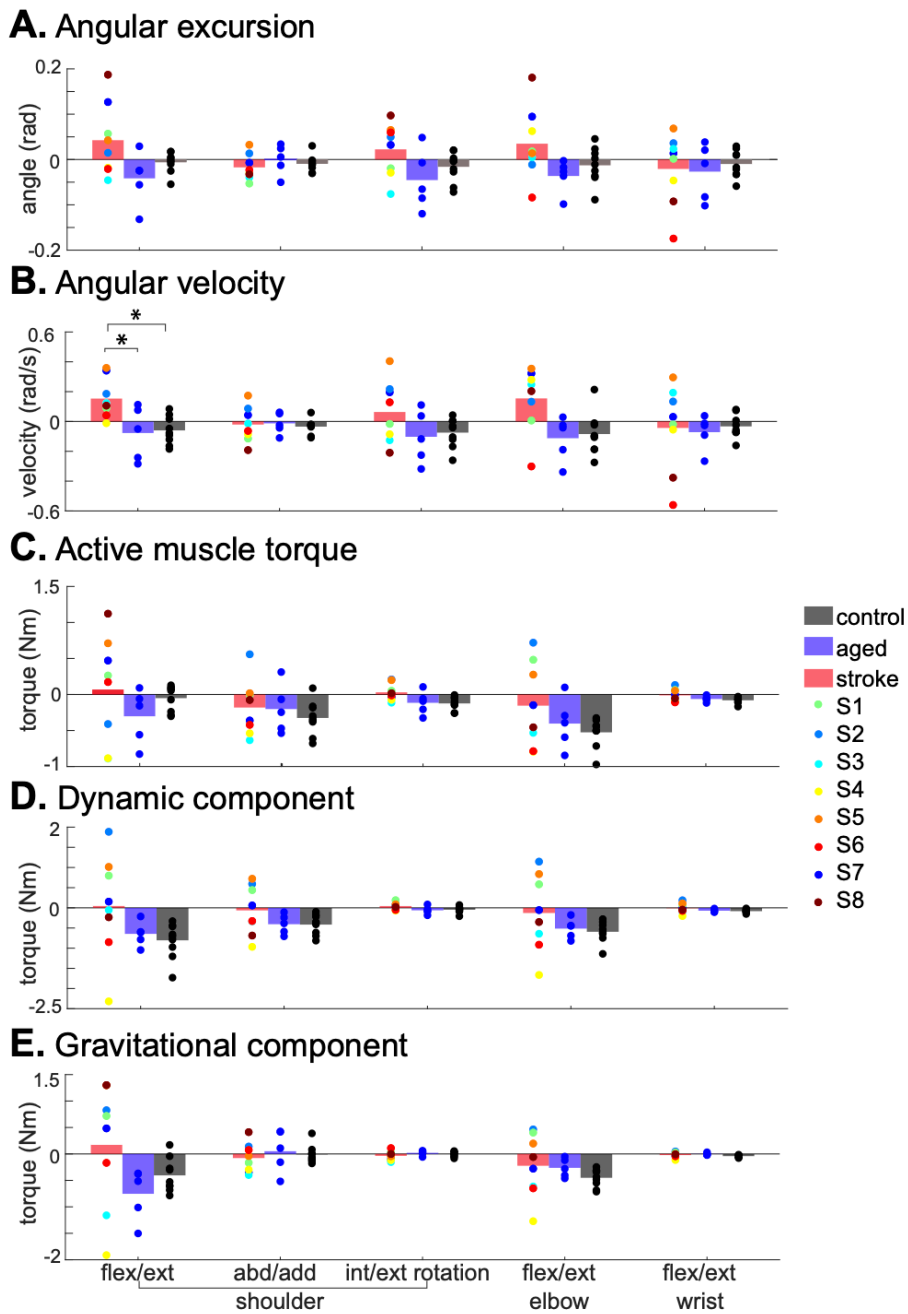

Supplementary Figure S1. Amplitude metric across limbs. Bars show the average difference between limbs across subjects; symbols show values for individual participants. Significantly different group comparisons due to non-overlapping confidence intervals from ANOVA model are marked by asterisks. The amplitude metric calculated based on angular excursions is shown in A, angular velocity in B, muscle torque in C, the gravitational component of muscle torque in D, and the dynamic component of muscle torque in E. Flex/ext indicates flexion and extension DOF, abd/add indicates abduction and adduction DOF, int/ext indicates internal and external rotation. Stroke group participant IDs match those in Table 1.

The repeated-measures ANOVA on the amplitude metric with contralesional vs. ipsilesional Stroke group comparisons had a significant effect of within-subject factors (F = 5.8, p = 0.005) and insignificant interaction with between-subject factor Group (F = 1.7, p = 0.159). Post-hoc comparisons between the levels of between- nor within-group factors were significant due to larger variability in the Stroke group data (Suppl. Table 1).

Supplementary Table 1: Post-hoc comparisons for ANOVA on amplitude metric across limbs, contralesional vs. ipsilesional for Stroke participants.

	Difference	Standard Error	*p*
A: Comparison between groups			
Aged – Control	0.002	0.098	1.000
Aged – Stroke	-0.163	0.100	0.259
Control – Stroke	-0.165	0.086	0.158
B: Comparison between DOFs			
Elbow F/E – Shoulder F/E	-0.044	0.045	0.859
Elbow F/E – Shoulder Ab/Ad	-0.107	0.039	0.082
Elbow F/E – Shoulder In/Ex	-0.192	0.054	0.016
Elbow F/E – Wrist F/E	-0.183	0.051	0.014
Shoulder F/E – Shoulder Ab/Ad	-0.063	0.063	0.849
Shoulder F/E – Shoulder In/Ex	-0.148	0.077	0.338
Shoulder F/E – Wrist F/E	-0.139	0.079	0.426
Shoulder Ab/Ad – Shoulder In/Ex	-0.085	0.029	0.053
Shoulder Ab/Ad – Wrist F/E	-0.075	0.033	0.202
Shoulder In/Ex rot – Wrist F/E	0.010	0.016	0.022
C: Comparison between signal types			
ANG - TORD	0.241	0.083	**0.**063
ANG - TORG	0.127	0.054	**0.**177
ANG - TORM	0.154	0.047	**0.**029
ANG - VEL	0.014	0.023	0.968
VEL - TORD	0.227	0.077	**0.**057
VEL - TORG	0.112	0.057	0.319
VEL - TORM	0.139	0.050	0.075
TORM - TORD	0.088	0.053	**0.**493
TORM - TORG	-0.027	0.029	0.883
TORD - TORG	-0.114	0.055	**0.**262

F/E stands for flexion/extension; Ab/Ad stands for abduction/adduction; In/Ex stand for internal/external rotation of the shoulder. The significant alpha corrected for repeated measures in A is equal to 0.0170; the corrected alpha in B and C is equal to 0.0051. ANG stands for angular excursions; VEL stands for angular velocity; TORM stands for muscle torque; TORD stands for the dynamic component of muscle torque; TORG stands for the gravitational component of muscle torque.

The intertrial metric described in Methods was also compared differently between limbs of the Stroke group participants. For the Control and Aged groups, the values for the non-dominant limb were subtracted from the values for the dominant limb as shown in Fig. 4. For the Stroke

group, the values for the limb contralesional to stroke (more affected) were subtracted from the values for the ipsilesional limb (less affected). Replotting the difference in intertrial variance between limbs in the Stroke group increased the intersubject variance in the metric based on the dynamic component of muscle torque (Suppl. Fig. S2; Fig. 4). The repeated-measures ANOVA on the intertrial variance metric had a significant effect of within-subject factors (F = 7.8, p = 2e-4) and insignificant interaction with between-subject factor Group (F = 0.9, p = 0.47). Post-hoc comparisons have shown that the amplitude metric was not significantly different between groups (Table 3A). Likewise, the differences between DOFs and signal types were insignificant (Table 3B, C). Therefore, handedness appears to be a better indicator of intertrial variance than post stroke deficits.

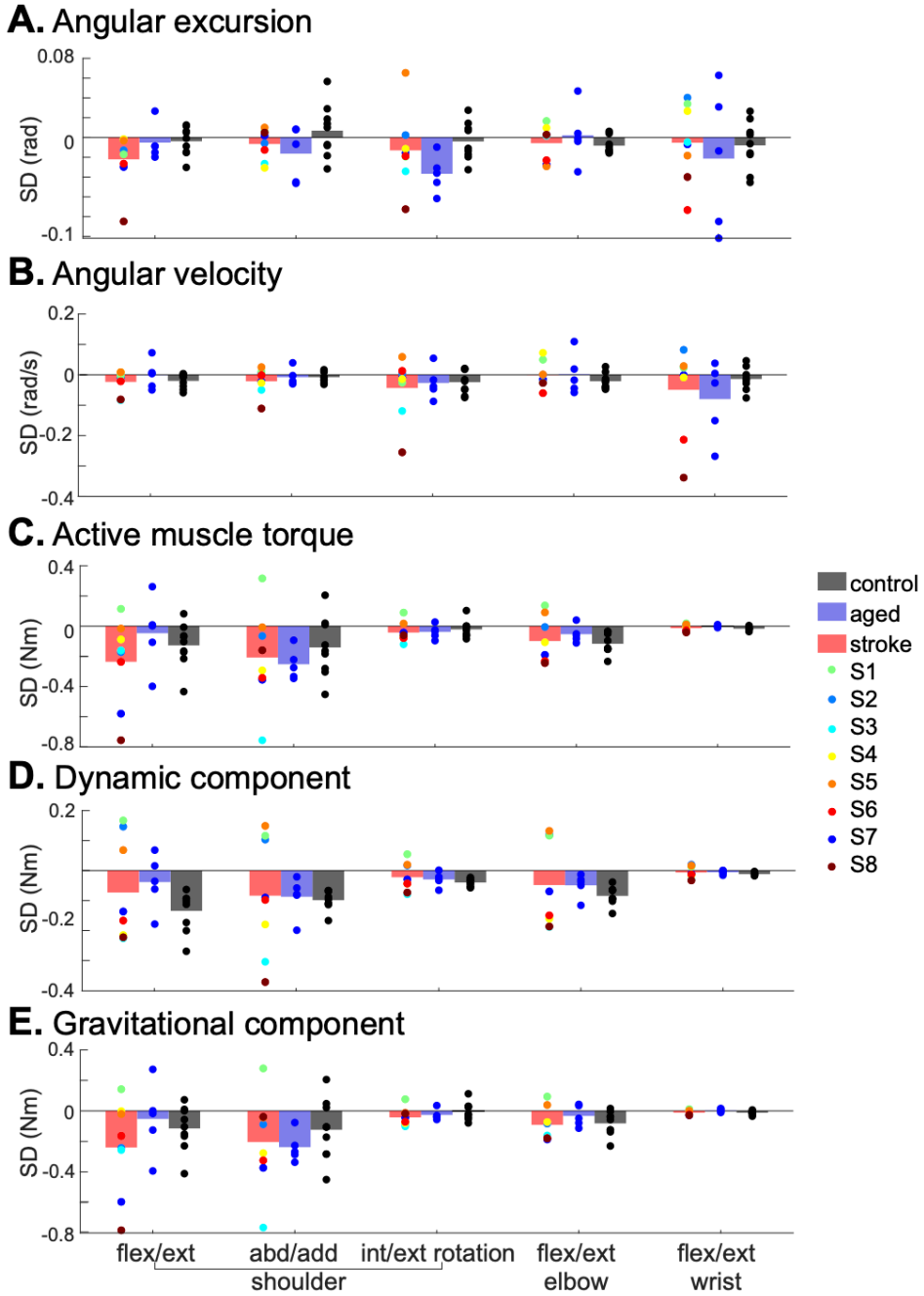

Supplementary Figure S2. Intertrial variance metric across limbs. The formatting of plots is as in Supplementary Figure S1.

Supplementary Table 2: Post-hoc comparisons for ANOVA on intertrial variance metric across limbs, contralesional vs. ipsilesional for Stroke participants.

	Difference	Standard Error	*p*
A: Comparison between groups			
Aged – Control	0.004	0.034	0.994
Aged – Stroke	0.019	0.035	0.852
Control – Stroke	0.015	0.030	0.866
B: Comparison between DOFs			
Elbow F/E – Shoulder F/E	0.030	0.019	0.519
Elbow F/E – Shoulder Ab/Ad	0.054	0.017	0.038
Elbow F/E – Shoulder In/Ex	-0.018	0.008	0.215
Elbow F/E – Wrist F/E	-0.029	0.009	0.043
Shoulder F/E – Shoulder Ab/Ad	0.024	0.024	0.860
Shoulder F/E – Shoulder In/Ex	-0.048	0.021	0.180
Shoulder F/E – Wrist F/E	-0.059	0.022	0.101
Shoulder Ab/Ad – Shoulder In/Ex	-0.072	0.019	0.008
Shoulder Ab/Ad – Wrist F/E	-0.083	0.024	0.017
Shoulder In/Ex rot – Wrist F/E	-0.011	0.007	0.615
C: Comparison between signal types			
ANG - TORD	0.044	0.015	0.056
ANG - TORG	0.075	0.020	0.009
ANG - TORM	0.085	0.021	0.006
ANG - VEL	0.013	0.008	0.493
VEL - TORD	0.032	0.013	0.171
VEL - TORG	0.062	0.018	0.020
VEL - TORM	0.072	0.019	0.009
TORM - TORD	-0.040	0.015	0.095
TORM - TORG	-0.010	0.005	0.290
TORD - TORG	0.030	0.017	0.384

F/E stands for flexion/extension; Ab/Ad stands for abduction/adduction; In/Ex stand for internal/external rotation of the shoulder. The significant alpha corrected for repeated measures in A is equal to 0.0170; the corrected alpha in B and C is equal to 0.0051. ANG stands for angular excursions; VEL stands for angular velocity; TORM stands for muscle torque; TORD stands for the dynamic component of muscle torque; TORG stands for the gravitational component of muscle torque.